VEGFC Reduces Glomerular Albumin Permeability and Protects Against Alterations in VEGF Receptor Expression in Diabetic Nephropathy

Karen L. Onions,[1] Monica Gamez,[1] Nicola R. Buckner,[1] Siân L. Baker,[1] Kai B. Betteridge,[1] Sara Desideri,[1] Benjamin P. Dallyn,[1] Raina D. Ramnath,[1] Chris R. Neal,[1] Louise K. Farmer,[1] Peter W. Mathieson,[1] Luigi Gnudi,[2] Kari Alitalo,[3] David O. Bates,[4] Andrew H.J. Salmon,[1] Gavin I. Welsh,[1] Simon C. Satchell,[1] and Rebecca R. Foster[1]

Diabetes 2019;68:172–187 | https://doi.org/10.2337/db18-0045

Elevated levels of vascular endothelial growth factor (VEGF) A are thought to cause glomerular endothelial cell (GEnC) dysfunction and albuminuria in diabetic nephropathy. We hypothesized that VEGFC could counteract these effects of VEGFA to protect the glomerular filtration barrier and reduce albuminuria. Isolated glomeruli were stimulated ex vivo with VEGFC, which reduced VEGFA- and type 2 diabetes–induced glomerular albumin solute permeability (Ps'alb). VEGFC had no detrimental effect on glomerular function in vivo when overexpression was induced locally in podocytes (podVEGFC) in otherwise healthy mice. Further, these mice had reduced glomerular VEGFA mRNA expression, yet increased glomerular VEGF receptor heterodimerization, indicating differential signaling by VEGFC. In a model of type 1 diabetes, the induction of podVEGFC overexpression reduced the development of hypertrophy, albuminuria, loss of GEnC fenestrations and protected against altered VEGF receptor expression. In addition, VEGFC protected against raised Ps'alb by endothelial glycocalyx disruption in glomeruli. In summary, VEGFC reduced the development of diabetic nephropathy, prevented VEGF receptor alterations in the diabetic glomerulus, and promoted both glomerular protection and endothelial barrier function. These important findings highlight a novel pathway for future investigation in the treatment of diabetic nephropathy.

Systemic endothelial dysfunction is an initiating step in the development of vascular damage in diabetes (1,2) and is associated with microalbuminuria (urinary albumin secretion 30–300 mg/day) (3). It is widely accepted that microalbuminuria indicates disruption of the glomerulus and is the earliest clinically detectable indicator of incipient diabetic nephropathy (DN) (4). Glomerular endothelial cells (GEnCs) restrict the passage of protein across the highly specialized glomerular capillary wall via the luminal facing endothelial glycocalyx (eGLX), which consists of proteoglycans, glycosaminoglycans (GAGs), glycoproteins, and trapped soluble plasma proteins. GEnCs have transcellular fenestrations that form in attenuated areas of GEnC cytoplasm, which constitute 20–50% of the entire endothelial cell surface (5). Fenestrae are necessary for the high permeability of the glomerulus to water and small solutes (5). However, fenestrae are covered by eGLX (6), which is known to regulate vascular permeability (7–10) by limiting the passage of charged macromolecules (11).

Vascular endothelial growth factor (VEGF) A is highly expressed by podocytes in the glomerulus (12) and provides essential maintenance signals for GEnC, including those for survival and regeneration (13), maintenance of fenestrations (14), and regulation of solute flux and protein passage (15,16). Systemic and glomerular vessels become more "leaky" in pathological conditions where

[1]Bristol Renal, Bristol Heart Institute, Translational Health Sciences, Bristol Medical School, University of Bristol, Bristol, U.K.
[2]School of Cardiovascular Medicine and Science, British Heart Foundation Centre of Excellence, King's College London, London, U.K.
[3]Wihuri Research Institute and Translational Cancer Biology Program, Biomedicum Helsinki, University of Helsinki, Helsinki, Finland
[4]Cancer Biology, Division of Cancer and Stem Cells, School of Medicine, University of Nottingham, Queen's Medical Centre, Nottingham, U.K.

Corresponding author: Rebecca R. Foster, becky.foster@bristol.ac.uk

Received 12 January 2018 and accepted 19 October 2018

This article contains Supplementary Data online at http://diabetes.diabetesjournals.org/lookup/suppl/doi:10.2337/db18-0045/-/DC1.

VEGFA bioavailability is increased, such as cancer, retinal disease (17), and early DN (18,19). Blockade of VEGFA in these experimental models reduces vascular permeability (20,21), including proteinuria in DN (6,22). However, clinical anti-VEGFA therapies (23–25) can cause proteinuria and hypertension (26), confirming that some VEGFA is necessary for endothelial maintenance. Therefore, strategies that block the adverse effects of excessive VEGFA, but do not remove it completely, would be attractive for DN.

VEGFC, a lymphangiogenic growth factor, is also expressed by podocytes (27), despite an absence of lymphatic vessels in glomeruli. VEGFC typically signals through VEGF receptor (VEGFR) 3, which is predominantly expressed in lymphatic endothelial cells, but can induce "maintenance" signals similar to those of VEGFA in vascular endothelial cells (28) acting through VEGFR3, VEGFR2, or heterodimers of both (29). VEGFC can also induce fenestration formations in the vascular endothelium, but to a lesser extent than VEGFA (30).

VEGFA predominantly signals through the phosphorylation of VEGFR2 (31). We have shown that VEGFA induces transient VEGFR2 phosphorylation after 2 min in human conditionally immortalized GEnCs (ciGEnCs) (32). VEGFC also induced VEGFR2 phosphorylation in these cells, maximally at 30 min, but did not induce VEGFR3 phosphorylation. VEGFC induced a correspondingly slower rise in intracellular calcium than VEGFA and did not result in vascular endothelial cadherin phosphorylation. We hypothesize that such differences in intracellular events underlie our observation that VEGFA increases the permeability of ciGEnC monolayers to protein, whereas VEGFC reduces protein permeability and blocks the effect of VEGFA (32). Additionally, VEGFC enhances the eGLX layer in vitro, in contrast to VEGFA, which increases eGLX shedding (32,33).

Together, these data suggest that VEGFC may be able to ameliorate albuminuria by reducing the permeability of GEnC to protein while retaining high water permeability. Thus, the effect of VEGFC on raised glomerular albumin permeability was assessed under various conditions, and VEGFC receptor signaling was explored. Finally, the mechanisms of VEGFC action on GEnC barrier properties were investigated with a specific focus on the eGLX.

RESEARCH DESIGN AND METHODS

Glomerular Endothelial Cell Culture

Human ciGEnCs were maintained and propagated in culture as described previously (34). ciGEnCs stably transfected with GFP (green fluorescent protein)-tagged VEGFR2 (ciGEnC/GFP-VEGFR2) (a gift from Dr. H. Mellor, University of Bristol, Bristol, U.K.) were cultured similarly.

Recombinant Proteins

Human recombinant VEGFA and VEGFC (R&D Systems) were reconstituted as done previously and were used at a final concentrations of 1 nmol/L (42 ng/mL) and 10 nmol/L (210 ng/mL), respectively, as described previously (32).

Antibodies

All primary and secondary antibodies that were used and their dilutions are described in Supplementary Table 1.

Immunofluorescence

Immunofluorescence was carried out on fresh frozen mouse kidney sections as previously described (35) and on GEnC as previously described (33). The integrated density of glomerular VEGFC was semiquantified using ImageJ (15 glomeruli per animal) and expressed as the fold change to littermate control (LMC) mice. For cellular VEGFR3 quantification, images were acquired using the InCell Analyzer 2200 System (GE Healthcare) as previously described (36). In brief, analysis was performed using the InCell Analyzer 1000 Workstation Multitarget analysis algorithms, using phalloidin to define the cell and DAPI to segment the nuclei. VEGFR3 is reported as the mean fluorescence intensity per cell.

Western Blotting

ciGEnCs, tissue, and sieved glomeruli and flow-through were lysed in radioimmunoprecipitation assay buffer containing phosphatase and protease inhibitors. Samples were quantified (Pierce bicinchoninic acid assay; Thermo Fisher Scientific) and Western blotted.

RNA Extraction and PCR

RNA was extracted from isolated mouse glomeruli using an RNeasy Mini Kit (Qiagen) according to manufacturer instructions. Primer sequences were predesigned, selected from http://pga.mgh.harvard.edu/primerbank/, and optimized as previously described (33). Human GAPDH primers were used as previously described (33), with other primer pairs described in Supplementary Table 2. Quantitative PCR was carried out as previously described (33). $2^{-\hat{}\hat{}CT}$ (relative fold change) was calculated from the CT values generated.

VEGFR3 Immunoprecipitation

Mouse lungs and glomeruli were freshly harvested in ice-cold PBS containing 100 μm of Na_3VO_4 and protease inhibitor cocktails (1:100) (Sigma-Aldrich). These tissues were then treated with VEGFA and VEGFC or vehicle at 37°C for 2, 15, or 30 min. PBS was removed, and samples were resuspended in 100 μL of NP-40 lysis buffer then precleared. Equal quantities of protein, to 500 μL, were incubated at 4°C for 18 h with 1.5 μg/100 μg protein of anti-mouse VEGFR3 (ALF4) (eBioscience). Subsequently, 60 μL of equilibrated A/G PLUS-agarose beads (Santa Cruz Biotechnology) were added to each sample and incubated at 4°C for 6 h. Beads were centrifuged, and supernatant samples were taken for immunoblotting. Thirty microliters of immunoprecipitation samples and equal protein concentrations of supernatant and total protein were loaded onto an SDS-PAGE gel and Western blotted.

Podocin Reverse Tetracycline-Controlled Transcriptional Activator, Tet-*O*-VEGFC (podVEGFC) Mice

Podocin reverse tetracycline-controlled transcriptional activator (podrtTA) mice expressing the transgene exclusively in podocytes (37) were a gift from Dr. J. Kopp (National Institutes of Health, Bethesda, MD) (FVB/mixed). Tet-*O*-VEGFC mice (FVB/N), containing full-length mouse VEGFC, were used as previously described (38). Heterozygous podrtTA mice were crossed with heterozygous Tet-*O*-VEGFC mice to obtain mice heterozygous for both transgenes (podVEGFC) and LMC mice. Animals were kept according to the *Guidelines on the Use of Animals in Research*, and the number of animals used was kept to a minimum. Mice were housed in a pathogen-free environment at 21°C, with a 12-h light/dark cycle, and all received a standard laboratory animal diet (Beekey Feeds) and water ad libitum.

Animal Genotyping

Ear notches were digested in 20-μL digestion buffer (1× PCR buffer [supplied with Hotmaster taq]: 0.0045% NP-40, 0.0045% Tween 20, 1 mg/mL proteinase K). Samples were digested for 2 h at 60°C, then for 15 min at 95°C. PCR for podrtTA was carried out as originally described (37). For Tet-*O*-VEGFC, primers are described in Supplementary Table 2. The PCR reaction (total volume 13 μL) contained 6.5 μL of Mastermix buffer (Amplitaq Gold 360; Applied Biosystems) and 0.5 μmol/L primers. PCR cycle conditions were as follows; 1 cycle at 95°C for 10 min, 42 cycles of 1 cycle at 95°C for 30 s, 68°C 30 s, 72°C for 60 s, and 72°C for 7 min.

Induction of Podocyte VEGFC Overexpression in Transgenic Mice

Expression of podocyte VEGFC was induced by doxycycline (2 mg/mL) in the drinking water with sucrose (5% w/v) as previously shown (37). Doxycycline was replaced every 3–4 days and protected from light at all times. If mice did not drink the doxycycline water, they received chow supplemented with 625 mg/kg doxycycline (Harlan Laboratories Ltd., Shardlow Derby, U.K.), which was observed to increase VEGFC mRNA expression to a similar extent (0.9-fold change in VEGFC mRNA expression compared with doxycycline-supplemented water; data not shown). Some animals were given sucrose alone. Urine samples were collected weekly in metabolic cages with environmental enrichment up to 6 h at a time.

Type 2 Diabetic Mice

Twelve- to 14-week-old male C57BLKsJ-*db*/*db* (*db*/*db*) mice (Harlan Laboratories Ltd.) were used as a model of spontaneous type 2 diabetes. Age-matched, male C57BLKsJ-*db*/+ (*db*/+) lean mice were used for comparison. mRNA was extracted from enriched glomeruli from 7-week-old *db*/*db* and *db*/+ mice. Urinary albumin/creatinine ratio (uACR) and glucose levels were measured as below.

Induction of Type 1 Diabetes

Diabetes was induced in 8- to 10-week-old podVEGFC and LMC mice using a low-dose (50 mg/kg/day over 5 consecutive days) streptozotocin (STZ) induction protocol as previously described (39) (as advised by Diabetic Complications Consortium [DiaComp], https://www.diacomp.org). Mice were checked for adverse effects after dosing; animals that demonstrated dehydration (including weight loss, slack skin, or bloating due to constipation, revealed postmortem in the first few diabetic mice) were supplemented with "mash" and DietGel with subcutaneous 0.9% saline injections as necessary. Blood glucose levels were monitored weekly from a tail-tip blood droplet using an Accu-Chek Blood Glucose Meter (Aviva). Animals with blood glucose >15 mmol/L 2 weeks after injections were included in the study. Body weight was monitored regularly. Mice received doxycycline from 0 weeks (prevention) or 4 weeks (rescue) after STZ administration. Urine was collected as previously described, although as animals became more polyuric, the collection time was reduced to minimize water weight loss and stress.

Glomerular Albumin Permeability Assay

This assay was developed and extensively characterized previously (40). In brief, mice were anesthetized and the kidneys perfused with 4% BSA (RingerBSA), followed by 36.5 μg/mL octadecyl rhodamine B chloride (R18) (Thermo Fisher Scientific) to label cell membranes, then 30 μg/mL Alexa Fluor (AF) 488-BSA (labeled albumin) (Life Technologies). Glomeruli were isolated from kidney cortex by graded sieving. For glomeruli treated ex vivo, glomeruli loaded with AF 488-BSA were held on ice until treated with VEGFA, VEGFC, both VEGFA and VEGFC, or an equal volume of Ringer-BSA (vehicle) for 1 h at 37°C. Individual glomeruli were transferred to a Nikon TIE Inverted Confocal Microscope and trapped before the perfusate was switched from 30 μg/mL AF 488-BSA to 30 μg/mL unlabeled BSA. The rate of decrease in fluorescence intensity within capillary loops was quantified, and from this apparent glomerular albumin solute permeability (Ps'alb) was calculated (40):

$$P_{S'alb} = -kR/2$$

In Vivo eGLX Disruption

We have shown previously that chondroitinase and hyaluronidase, given acutely i.v. 30 min before sacrifice, raises Ps'alb significantly and causes a reduction in eGLX coverage (40). In the same cohort of animals, glomeruli were isolated and incubated in VEGFC as described above, and Ps'alb level was measured and compared. Further, chondroitinase and hyaluronidase were administered chronically, via an osmotic minipump (0.25 μL/h) (Charles River UK Ltd., Kent, U.K.), and cannulated to the jugular, for a total of 2 weeks (0.087 mU/g chondroitinase and 15 mU/g hyaluronidase, or vehicle over a 24-h period, equivalent to 0.004 mU/h chondroitinase and 0.625 units/h hyaluronidase). In the final week, a VEGFC intervention was given to half of the enzyme-treated mice i.p. daily

(100 ng/g body wt as previously described) (41). Glomeruli were isolated, and Ps'alb was measured.

Electron Microscopy

Mice were whole-body perfusion fixed with glutaraldehyde containing Alcian blue. Electron micrographs were taken using a Technai 12 Electron Microscope, and images were analyzed as previously described (39).

uACR

Mouse uACRs were quantified as previously described (39) and expressed as the log fold change from baseline.

Glomerular Isolation

To achieve a >97% pure population of isolated glomeruli, Dynabeads were cardiac perfused as originally described by Takemoto et al. (42) and placed in RNA later (Invitrogen). Alternatively, to obtain a glomerular enriched population, kidneys were mashed, and glomeruli isolated through graded sieving and collected from 75-μm^2 pore sieves for protein or mRNA extraction. To demonstrate glomerular enrichment, kidney cortex, flow-through, and sieved glomeruli were collected, and lysates were extracted, quantified, and Western blotted as described above. Blots were probed with anti-nephrin, anti-CD13, and anti-actin antibodies (Supplementary Table 1).

Proximity Ligation Assay

Fresh frozen mouse kidney sections were fixed in 4% paraformaldehyde and permeabilized using 0.1% Triton X-100. Samples were then treated with the Proximity Ligation Assay Kit (Olink Bioscience) according to the manufacturer instructions. In brief, primary antibodies or matched concentration IgG controls in various combinations were incubated together overnight (for details, see Supplementary Table 1), followed by incubation with goat MINUS and rabbit PLUS probes. Nuclei were counterstained using DAPI (1:1,000 diluted in proximity ligation assay (PLA) kit 0.01× wash buffer B). Images were quantified by a blinded analyzer using ImageJ, by counting the number of punctate dots through *z*-stacks of images and normalizing to the number of nuclei within the field of view. Three representative *z*-stacks from each sample were analyzed.

Periodic Acid-Schiff Staining of Mouse Kidney Sections

Paraffin-embedded mouse kidney sections were stained using a periodic acid-Schiff (PAS) kit (Sigma-Aldrich) according to the manufacturer instructions. Six glomerular images were analyzed per mouse and quantified as previously described (40).

Picro Sirius Red Staining

Mouse tissue sections were hydrated followed by counterstaining in a 0.1% (w/v) Direct Red 80 powder (Sigma-Aldrich) in a 1.3% saturated aqueous solution of picric acid (VWR Chemicals) for 90 min at room temperature, then dehydrated and mounted. Images were taken using a bright-field (to indicate collagen I and III) and a polarized lens (to distinguish between type 1 (yellow-orange) and type 3 (green-white) newly laid collagen fibers).

Statistical Analysis

All statistical analysis was carried out on a minimum of three separate experiments. In Ps'alb experiments, data are presented as the means of measurements from glomeruli to show the spread of data points, but for statistical purposes the means from individual animals were used. In experiments with multiple treatments, a one-way ANOVA was used with Bonferroni's multiple-comparison post hoc test, unless indicated otherwise. A P value of less than 0.05 was considered statistically significant. Error bars indicate the SD.

RESULTS

VEGFC Prevents the Increase in Ps'alb Caused by VEGFA and Type 2 Diabetes and Is Cytoprotective for GEnCs

To test whether VEGFC could protect against the effects of raised VEGFA, an ex vivo isolated glomerular Ps'alb assay was used that we recently published (40). VEGFA significantly increased Ps'alb in isolated glomeruli as anticipated in the FVB/mixed background (Fig. 1*A*) and *db*/− (lean) mice (Fig. 1*B*). Importantly, this effect was prevented by VEGFC, yet VEGFC alone did not change Ps'alb. To understand whether VEGFC could rescue Ps'alb induced by diabetes, glomeruli were isolated from *db*/*db* (type 2 diabetic) mice and stimulated with VEGFC ex vivo, as described above. Ps'alb in diabetic glomeruli was significantly raised, as anticipated, whereas it was significantly rescued by VEGFC (Fig. 1*C*). *db*/*db* mice were 12–14 weeks old, had significant proteinuria (Fig. 1*D*), and were hyperglycemic (Fig. 1*E*). We confirmed that there was a significant increase in VEGFA mRNA expression in enriched glomeruli from *db*/*db* mice (Fig. 1*F*). We also confirmed that VEGFC was cytoprotective for GEnCs, an important protective effect of VEGFA. Using a Trypan Blue viability assay, we determined that GEnCs were protected from death (serum free, volume reduced media) by VEGFC over 24 h in a manner similar to that by VEGFA (Supplementary Fig. 1*A*). This was associated with increased Akt phosphorylation over time by VEGFC and VEGFA (Supplementary Fig. 1*B*), suggesting that VEGFC promotes survival in GEnCs in a manner similar to VEGFA in vitro.

Characterization of podVEGFC Mice

To determine whether VEGFC could be protective in vivo, we generated a podVEGFC mouse (Fig. 2*A*). First, glomeruli were Dynabead isolated from podVEGFC and LMC mice after receiving doxycycline for 3 weeks. Quantitative PCR revealed a significant increase in normalized VEGFC glomerular mRNA expression in podVEGFC mice (Fig. 2*B*). This was supported by immunofluorescence showing colocalization of VEGFC with nephrin (Fig. 2*C*) in podVEGFC mice.

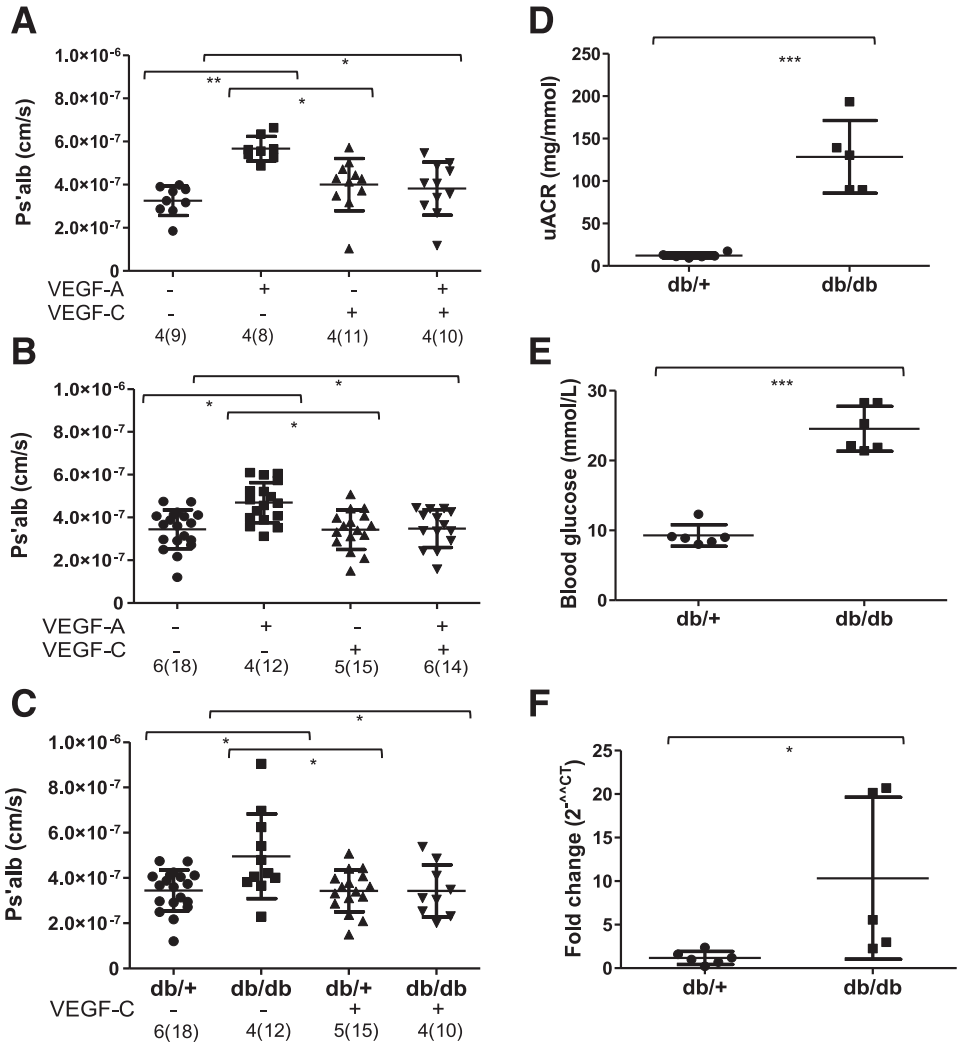

Figure 1—VEGFC prevents the increase in glomerular Ps'alb caused by VEGFA and type 2 diabetes. Glomeruli were sieved from healthy mice (FVB/mixed background [*A*] and *db*/+ lean control [*B*]) and stimulated ex vivo with vehicle, 1 nmol/L VEGFA, 10 nmol/L VEGFC, or both for 1 h at 37°C, and Ps'alb was measured (one-way ANOVA with Bonferroni post hoc tests indicated). *C*: Glomeruli were sieved from *db*/+ and *db*/*db* mice at 12–14 weeks of age and were incubated ex vivo with (+) or without (−) VEGFC, then Ps'alb was measured (one-way ANOVA with Bonferroni post hoc tests are indicated). The number of animals is indicated outside brackets and number of glomeruli indicated inside brackets. uACR (*D*) and blood glucose (*E*) levels are shown for *db*/+ and *db*/*db* mice at 12–14 weeks of age. *F*: Fold change in VEGFA mRNA expression in sieved glomeruli from *db*/+ and *db*/*db* mice is shown (n = 6 and 5, respectively). $^*P < 0.05$, $^{**}P < 0.01$, $^{***}P < 0.001$.

Semiquantification demonstrated significantly increased glomerular protein expression in podVEGFC mice (Fig. 2*D*). Levels of VEGFC mRNA were similar in glomeruli isolated by Dynabead and sieving protocols (data not shown); therefore, sieving was used to isolate glomeruli hereafter.

VEGFC Has No Detrimental Effect on Glomerular Function

Glomerular parameters in podVEGFC mice were compared with LMC mice. There was no renal hypertrophy (Fig. 2*E*), mesangial matrix expansion (Fig. 2*Fi* and *G*), or ultrastructural changes in GBM thickness, podocyte foot process width, slit diaphragm length (Fig. 2*Fii* and *H*), fenestration density (Fig. 2*I*), or uACR (Fig. 2*J*) up to 8 weeks after the induction of VEGFC expression. Together, these results demonstrate that VEGFC does not significantly affect glomerular structure or function over prolonged periods of exposure, in contrast to VEGFA (43).

Glomerular VEGFC Expression Affects VEGF Signaling

Glomerular sieving successfully enriched the glomeruli population (Supplementary Fig. 2). In podVEGFC mice, there was a trend toward a reduction in VEGFR2 in the glomerular enriched fraction (Fig. 3*A*), but no significant reduction in VEGFR3 mRNA expression (Fig. 3*B*). VEGFA mRNA expression was significantly reduced (Fig. 3*C*). In nonpermeabilized cells, both VEGFA and VEGFC reduced cell surface VEGFR3 expression at 2 min (Fig. 3*D*), whereas total VEGFR2 and VEGFR3 expression was unaffected by VEGFA or VEGFC at 2 min (Supplementary Fig. 3). VEGFR3 and VEGFR2 heterodimerization by VEGFC, as

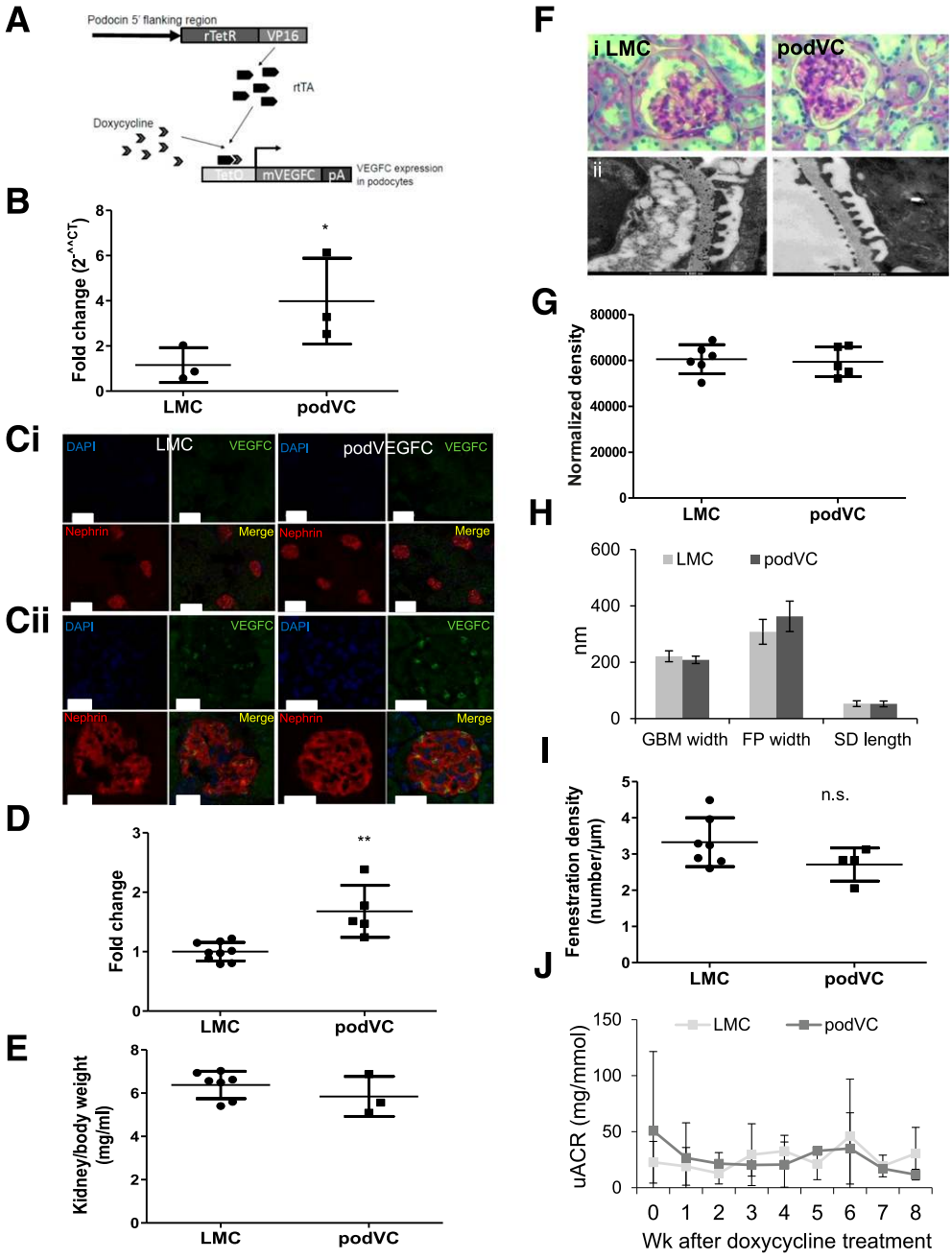

Figure 2—Characterization of podVEGFC mouse. *A*: A 2.5-kb fragment of the NPHS2 promoter-enhancer region directs the expression of rtTA in podocytes. In the presence of doxycycline, a transcriptional activator fusion protein binds to the tetracycline-response operon promoter element (TetO) and initiates mouse VEGFC transcription (29). *B*: Glomeruli were isolated from podVEGFC (podVC) or LMC mice after receiving doxycycline for 3 weeks. mRNA was extracted and quantitative PCR performed for VEGFC, normalized to GAPDH and to LMC animals ($2^{-\wedge\wedge CT}$) (*$P < 0.05$, unpaired *t* test, $n = 3$). *C*: Kidneys from LMC and podVEGFC mice on doxycycline for 8 weeks were removed and snap frozen, and coimmunofluorescence was performed with anti-VEGFC (green), anti-nephrin (red) antibody, and DAPI (blue). Representative confocal images are shown. Images are shown at 10× (*Ci*; scale bar, 25 μm) and ×40 (*Cii*; scale bar, 70 μm). *D*: Semiquantification was performed on glomeruli (VEGFC/DAPI) and presented as the fold change (**$P < 0.01$, unpaired *t* test; $n = 9$ and 5, respectively). *E*: Kidneys from LMC and podVEGFC mice given doxycycline for 8 weeks were weighed and expressed as a ratio to total body weight. PAS staining and ultrastructural changes were imaged (*Fi* and *Fii*). *Fi*, magnification = ×40; *Fii*, scale bar = 500 nm. PAS staining was quantified (*G*; n = 5 and 8) as were parameters of glomerular ultrastructure, including GBM width, podocyte foot (FP) process width, slit diaphragm (SD) length (*H*; n = 4 and 8) and fenestration density per micrometer of GBM length (*I*; n = 4 and 8). *J*: Weekly urine uACRs are expressed (n = 6 and 5).

reported previously (29,44), was investigated ex vivo in isolated glomeruli using immunoprecipitation. VEGFR2 was not pulled down by VEGFR3 in response to VEGFC (Fig. 3*E*). However, heterodimers were formed in response to VEGFC in mouse lungs as anticipated (Fig. 3*F*). Nilsson et al. (29) demonstrated that a PLA was more sensitive to

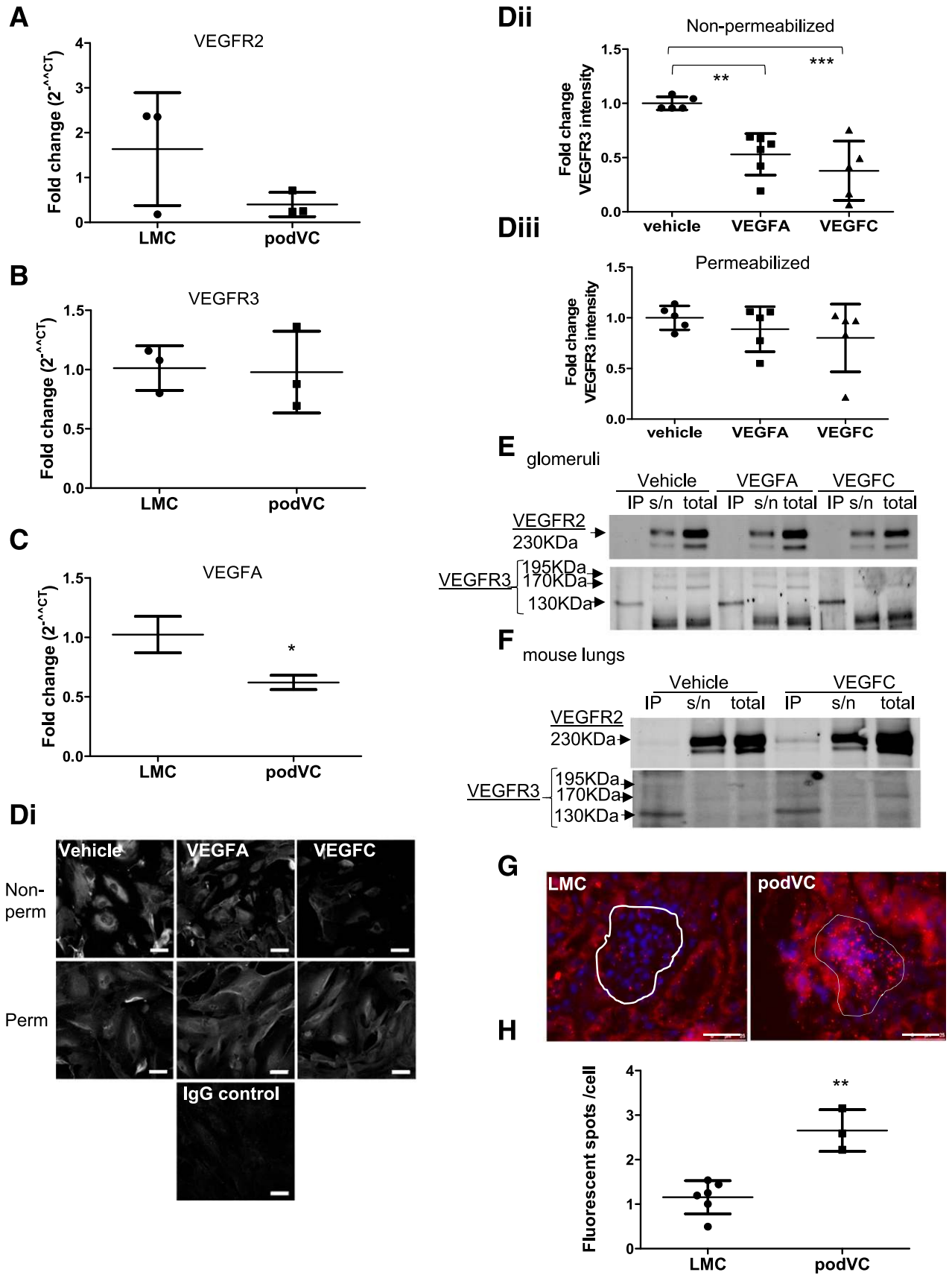

Figure 3—VEGFC overexpression affects VEGFA and VEGF receptors. Glomeruli were enriched from podVEGFC and LMC mice. Quantitative PCR was performed and normalized to GAPDH and LMC mice ($2^{-\Delta\Delta CT}$). Relative VEGFR2 (*A*), VEGFR3 (*B*), and VEGFA (*C*) mRNA expression is shown ($n = 3$; $^*P < 0.05$, unpaired *t* test). *D*: Human GEnCs were stimulated with VEGFC or VEGFA for 2 min; then fixed,

detect VEGFR2/VEGFR3 heterodimerization than immunoprecipitation. Thus, a PLA was used on fresh frozen sections from podVEGFC and LMC mice (Fig. 3*G*). Optimization, by replacing primary antibodies with matched concentration IgG, demonstrated the specificity of punctate staining (Supplementary Fig. 4). There was a significant increase in punctate fluorescent events, indicating heterodimerization, throughout the *z*-stacks of each glomerular cell in podVEGFC mice compared with LMC mice (Fig. 3*H*).

Early Glomerular VEGFC Expression Reduces the Development of DN

Endothelial dysfunction develops early in diabetes and manifests as microalbuminuria in the kidney. We have shown that VEGFC ameliorates raised Ps'alb associated with type 2 diabetes in isolated glomeruli. To understand whether VEGFC could prevent albuminuria in DN, doxycycline was administered before STZ injections (Fig. 4*A*). Diabetic mice (D-) were hyperglycemic (Fig. 4*B*), and had reduced body weight (Fig. 4*C*) and increased urine output (Fig. 4*D*), as anticipated. D-podVEGFC mice did not have significant renal hypertrophy (Fig. 4*E*) and had a significantly reduced fold change in uACR compared with D-LMC mice (Fig. 4*F*) (please refer to Supplementary Fig. 5*A* for absolute values), which was high but variable because of the mixed background of the mice. Diabetes did not significantly increase glomerular basement membrane (GBM) thickness or podocyte foot process width (Fig. 4*G* and *H*). However, podocyte slit diaphragm narrowing was evident in D-LMC mice (Fig. 4*G* and *H*). D-LMC mice had significantly lower endothelial fenestration density than LMC mice, whereas D-podVEGFC mice did not (Fig. 4*G* and *I*).

Glomerular VEGFC Intervention Reduces the Development of DN

To understand whether VEGFC could rescue DN after diabetes was established, doxycycline was administered 4 weeks after STZ injections (Fig. 5*A*). Diabetic mice were hyperglycemic (Fig. 5*B*) and polyuric (Fig. 5*C*), as anticipated. There was no significant difference in weight gain between groups; however, these diabetic mice were susceptible to intestinal bloating, which was likely to mask body weight reductions (this protocol was carried out chronologically before the one described above, and this issue was mitigated as described in RESEARCH DESIGN AND METHODS) (Fig. 5*D*). Of note, this cohort of mice also had a lower starting weight than the intervention cohort in Fig. 4, and sham mice did not gain weight as rapidly, which may confound the results. Elevated plasma uric acid level is associated with diabetes and can be caused by hyperglycemia (45). Plasma uric acid was significantly raised in both diabetic groups, as anticipated (Fig. 5*E*). Importantly, renal hypertrophy (Fig. 5*F*) was significantly increased in D-LMC mice, but significantly reduced in D-podVEGFC mice. The fold change in uACR (Fig. 5*G*) (please refer to Supplementary Fig. 5*B* for absolute values) was significantly increased in D-LMC mice but not in D-podVEGFC mice. Mesangial matrix expansion was significantly reduced in D-podVEGFC mice (Fig. 5*H* and *K*), supported by decreased collagen deposition (Fig. 5*I* and *J*). There was no significant effect of diabetes on GBM thickness, which is consistent with an early phenotype of DN (Fig. 6*A* and *B*). D-LMC mice had significantly increased podocyte foot process width, and both D-LMC and D-podVEGFC mice had significantly reduced slit diaphragm width (Fig. 6*B*). D-LMC mice also had significantly reduced fenestration density (Fig. 6*C*), demonstrating the early development of DN. Together, these data from both diabetic cohorts suggest that early VEGFC intervention may reduce the development of early DN.

Glomerular VEGFC Prevents the Diabetes Associated Changes in VEGFR Expression

The induction of VEGFC expression was confirmed in glomerular fractions from D-podVEGFC mice (Fig. 7*A*) in a manner similar to that from podVEGFC mice. There was no significant change in endogenous glomerular fractions of VEGFC expression between D-LMC and sham-LMC mice (Fig. 7*B*). VEGFA mRNA from glomerular fractions was increased by diabetes (Fig. 7*C*), as previously shown (46), with a trend toward an increase in D-podVEGFC mice (Fig. 7*C*). VEGFR2 and VEGFR3 mRNA from glomerular fractions were significantly increased in D-LMC mice, but not in D-podVEGFC mice (Fig. 7*D* and *E*). This was supported by VEGFR2 protein analysis, whereby VEGFR2 expression was significantly reduced in D-podVEGFC mice (Fig. 7*F* and *G*). Of note, VEGFR2 protein was undetected in sieved flow-through fractions (Supplementary Fig. 2*E*), suggesting that VEGFR2 protein changes were glomerular specific. VEGFR3 protein analysis was not significant (Fig. 7*F* and *H*). In summary, VEGFC prevented VEGFR changes associated with DN.

VEGFC Protects Against Raised Ps'alb Caused by Systemic eGLX Dysfunction

We have previously shown that VEGFC increases the synthesis of sulfated and nonsulfated GAGs in GEnC-GLX

nonpermeabilized or permeabilized, and stained for VEGFR3 or IgG control (scale bar, 50 μm). *Di*: Representative images are shown. Fold change in mean fluorescent intensity of VEGFR3 per cell is shown for nonpermeabilized (*Dii*) and permeabilized (*Diii*) GEnCs (n = 5–6; $P < 0.001$, one-way ANOVA). Isolated glomeruli (*E*) and homogenized lung (*F*) from wild-type mice were treated ex vivo with vehicle, VEGFC (30 min), and VEGFA (2 min, glomeruli fractions only). Samples were immunoprecipitated with anti-VEGFR3 then probed with anti-VEGFR3 or anti-VEGFR2. These are representative blots from three separate experiments. *G*: A PLA was performed on fresh frozen kidney sections from LMC or podVEGFC mice using antibodies to VEGFR2 and VEGFR3 (scale bar, 25 μm). *H*: Punctate events were counted through *z*-stacks in glomeruli (outlined) and expressed per nuclei. $^{*}P < 0.05$, $^{**}P < 0.01$, $^{***}P < 0.001$, unpaired t test, n = 6 and 3.

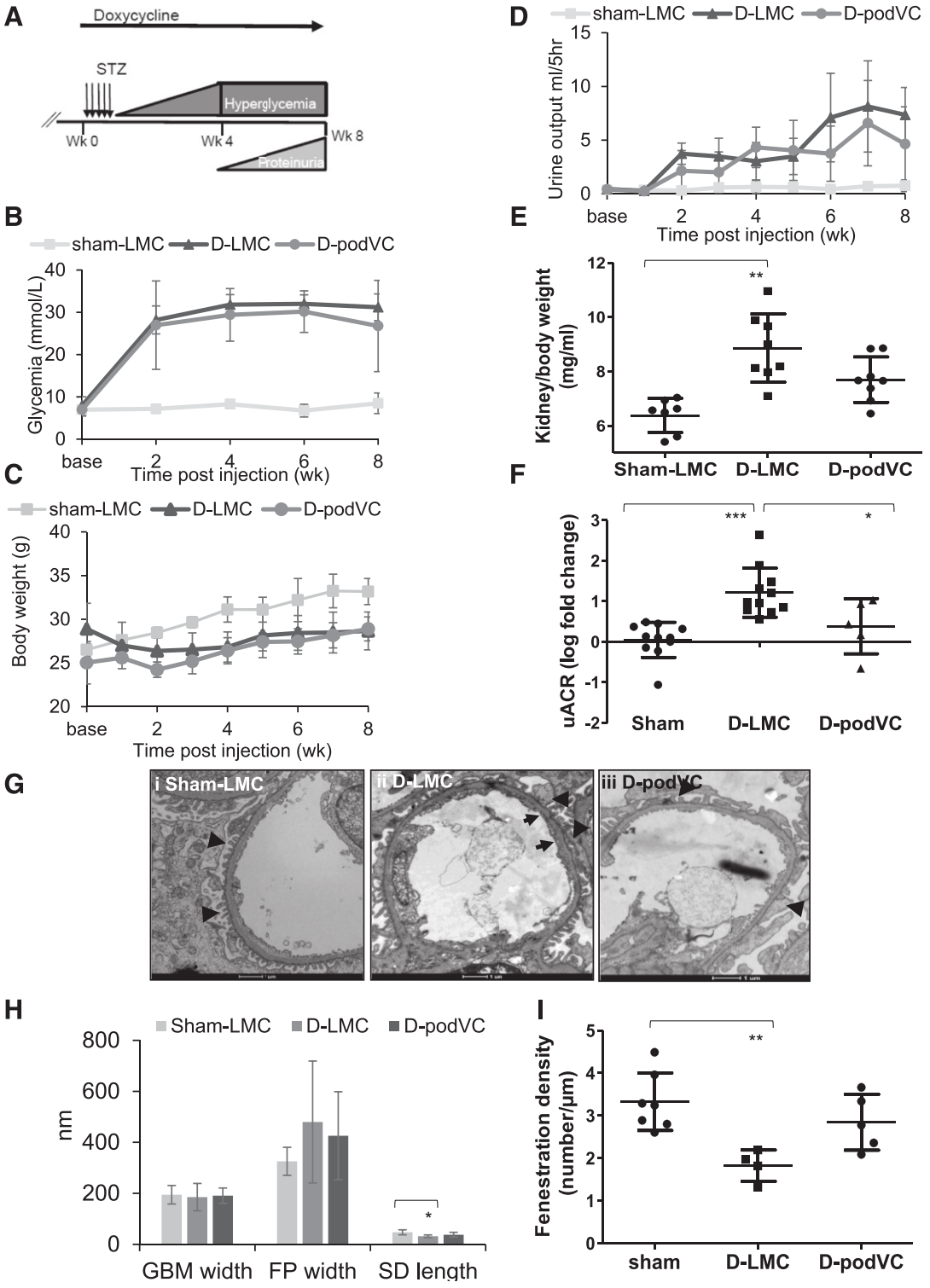

Figure 4—Early VEGFC expression reduces the development of DN. *A*: Mice were given doxycycline at the same time as STZ injections, at week 0. Glycemia (*B*), body weight (*C*), urine output (*D*), and kidney/body weight ratio (*E*; $P < 0.05$, one-way ANOVA) were monitored weekly after injections in D-LMC (diabetic) and D-podVEGFC mice compared with sham-LMC mice (n = 11, 3, and 5). *F*: Log fold change from baseline in uACR is shown at 8 weeks after STZ injection ($P < 0.05$, one-way ANOVA, n = 11, 11, and 5, respectively). Mice were cardiac perfusion fixed. Representative electron micrographs are shown at high power to show details of capillary loops in sham-LMC (*Gi*), D-LMC (*Gii*), and D-podVEGFC (*Giii*) mice. Arrows highlight the reduced endothelial fenestration density, and arrowheads highlight flattened foot processes. Scale bars, 1 μm. *H*: Ultrastructural changes were quantified by measuring GBM width, podocyte foot process (FP) width ($P < 0.05$, one-way ANOVA), and slit diaphragm (SD) length (n = 7, 4, and 5, respectively; $P < 0.001$, one-way ANOVA). *I*: Endothelial fenestration density per μm of GBM was also quantified (n = 7, 4, and 5, $P < 0.05$, one-way ANOVA). Bonferroni post hoc tests are indicated; $^*P < 0.05$, $^{**}P < 0.01$, $^{***}P < 0.001$, n = 5, 3, and 4. D-podVC, D-podVEGFC.

in vitro (33). Since macromolecular barrier properties in GEnCs are governed by eGLX (47), we investigated the potential for VEGFC to reduce Ps'alb in an eGLX-dependent manner. Previously, we demonstrated that a bolus of hyaluronidase and chondroitinase 30 min before sacrifice significantly reduced eGLX coverage and significantly increased Ps'alb (40). In the same cohort of mice, isolated glomeruli were stimulated with VEGFC for 1 h. In these glomeruli, VEGFC rescued the effect of eGLX disruption on Ps'alb (Fig. 8*A*). We followed this experiment with chronic, systemic exposure to these enzymes (2 weeks) with VEGFC i.p. injections given in the last week. Enzymes significantly increased Ps'alb in isolated glomeruli. However, this was significantly prevented in glomeruli from mice given the VEGFC intervention (Fig. 8*B*). Electron micrographs from mice in parallel experiments demonstrated that GAG enzymes significantly reduced GEnC eGLX depth, but not in the presence of VEGFC (Fig. 8*C* and *D*). Interestingly, podocyte glycocalyx was relatively unaffected (Fig. 8*D*). To demonstrate no off-target effects of the GAG enzymes, glomerular ultrastructural parameters were measured. There were no significant effects of enzymes on GBM width (although the combination of enzymes plus VEGFC significantly reduced GBM width), slit diaphragm width, podocyte foot process density (Fig. 8*E*) (although there was a significant overall effect), or endothelial fenestration density (Fig. 8*F*). In summary, VEGFC can protect from increased Ps'alb under eGLX dysfunction, suggesting the possibility that VEGFC protection from albuminuria is eGLX dependent.

DISCUSSION

In this study, we demonstrate for the first time that VEGFC can protect against VEGFA-induced Ps'alb and can restore Ps'alb in type 2 diabetes. Also, it can ameliorate early DN in type 1 diabetes; reducing fibrosis, kidney hypertrophy, loss in glomerular endothelial fenestration density, and albuminuria. There was an 89% reduction in albuminuria when VEGFC was used preventatively and a 67% reduction when VEGFC was used to rescue changes. These were comparable to previously published results demonstrating that glomerular overexpression of angiopoietin-1 in diabetic mice caused a 70% reduction in albuminuria (48) and glomerular overexpression of $VEGFA_{165}b$ in diabetic mice caused an 80% reduction in albuminuria (49). That VEGFC reversed the increased Ps'alb in type 2 diabetic glomeruli confirms the effect of VEGFC across mouse strains and diabetes type. This demonstrates that VEGFC can act as an antialbuminuric agent in experimental DN.

Diabetes-induced damage to glomerular ultrastructure included foot process flattening and reduced endothelial fenestration density (39,50,51). Reduced fenestration density is an established feature of DN in humans, which is positively correlated with uACR (51). It has been suggested that loss of GEnC fenestration density reflects both glomerular filtration rate and uACR better than changes in podocyte parameters (52). Of note, we did not see any changes in GBM thickness. This is surprising, but may be a reflection that podocyte damage is not yet severe enough to impact maintenance of the GBM (53) or may simply be a reflection of a mixed strain background. Notably, the D-podVEGFC mice did not have significantly reduced fenestration density. It is well established that GEnC fenestration density is reduced in DN. Fenestrations are too large to restrict albumin passage; however, the loss of fenestration density, or organization, may reflect a loss of filtration control. Also, renal hypertrophy was reduced in D-podVEGFC mice. Although our mice have early DN, they also have evidence of fibrosis, demonstrated by glomerular PAS staining and increased glomerular and tubular collagen I and III deposition, as is predicted in diabetes (54). Kidney weight is partially reduced in the D-podVEGFC mice. This may indicate a reduction in early fibrosis as a result of reduced albumin filtration and therefore reduced tubular toxicity (55).

We suggest that the differing effects between VEGFC and VEGFA may be due to differential activation of VEGFR2. We have previously shown that VEGFC does not induce VEGFR3 phosphorylation in ciGEnCs, yet promotes delayed VEGFR2 phosphorylation at 30 min compared with rapid phosphorylation by VEGFA at 2 min (32). However, we show that VEGFC causes rapid loss of cell surface VEGFR3 expression, suggesting internalization of VEGFR3 by VEGFC. In otherwise healthy glomeruli, chronic glomerular VEGFC expression induced VEGFR2 and VEGFR3 heterodimerization and reduced glomerular VEGFA mRNA expression without inducing glomerular fibrosis or a loss of glomerular function or changes in glomerular ultrastructure. This is important since reduced glomerular VEGFA expression can lead to renal thrombotic microangiopathy and proteinuria (26,43), yet increased glomerular VEGFA expression can lead to collapsing glomerulopathies and proteinuria (43). That VEGFC has no detrimental effect on glomerular function is fundamentally important to future studies aiming to manipulate the VEGFC pathway in order to protect glomeruli. It is known that VEGFC induces VEGFR2/VEGFR3 heterodimerization in lymphatic endothelial cells (44). Here, we demonstrate that chronic exposure to VEGFC induces heterodimerization in glomeruli. Also, glomerular VEGFA expression is repressed, similar to when Ang-1 is overexpressed (56), potentially altering receptor availability to VEGFC and thus facilitating heterodimerization. Interestingly, heterodimerization of VEGFR3 with VEGFR2 leads to reduced phosphorylation of some tyrosine sites in lymphatic endothelial cells (44). These results suggest that VEGFR3 is involved in VEGFC signaling, confirm functional activity of overexpressed VEGFC, and demonstrate for the first time in vivo that mouse VEGFC induces VEGFR2/VEGFR3 heterodimerization. Thus, the change in glomerular VEGFR complex formation may explain the different temporal effects on VEGFR2 phosphorylation

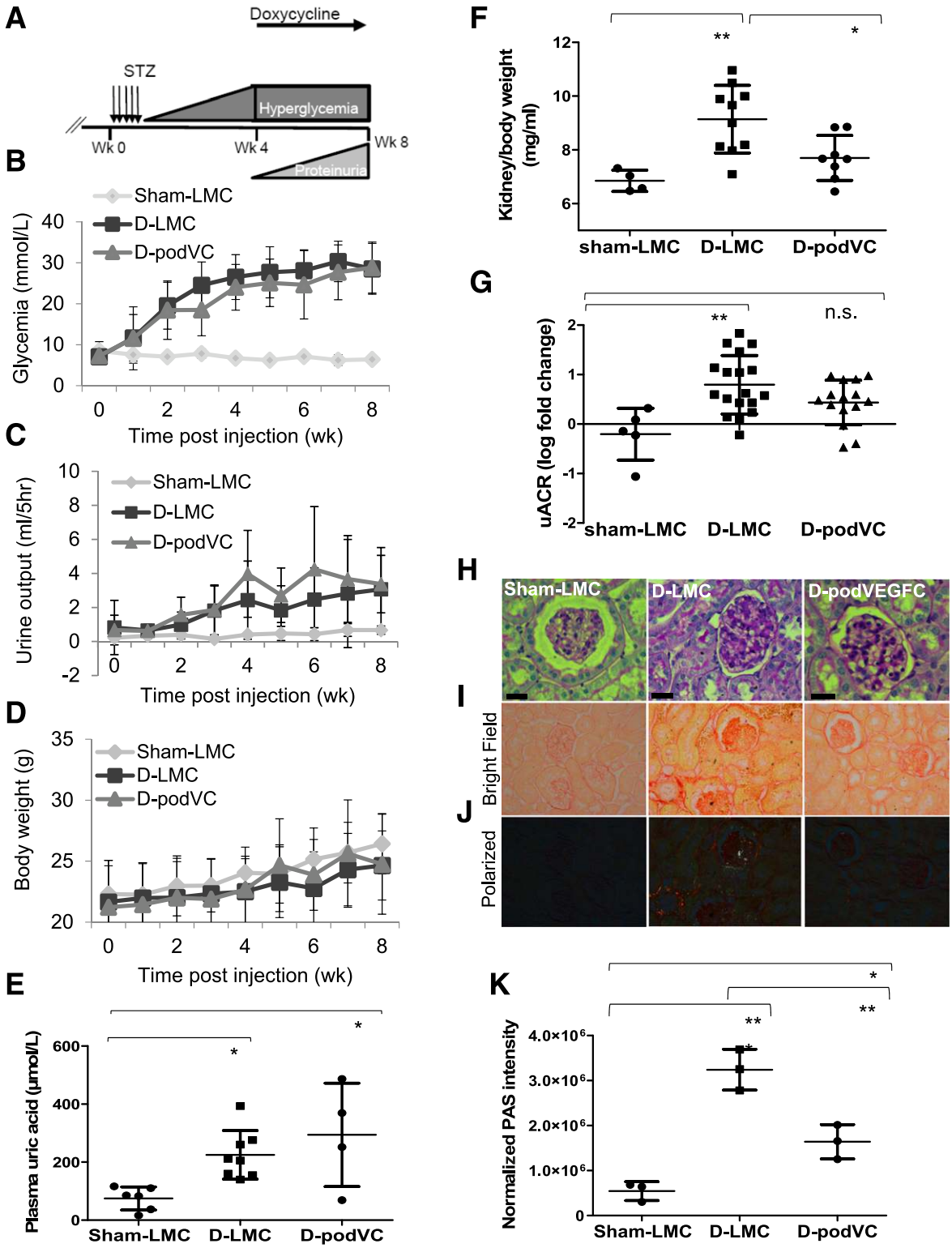

Figure 5—VEGFC intervention reduces the development of DN. *A*: Mice were given STZ injections at week 0, then were given doxycycline after the establishment of hyperglycemia at week 4. Glycemia (*B*; $n = 4$, 20, and 9), urine output (*C*; $n = 4$, 16, and 11), and body weight (*D*; $n = 4$, 20, and 9) were measured weekly in sham-LMC, D-LMC, and D-podVEGFC (D-podVC) mice. Plasma uric acid (*E*; $P < 0.05$, one-way ANOVA), kidney/body weight ratio (*F*; $P < 0.05$, one way ANOVA, $n = 4$, 10, and 9), and uACR, presented as the log fold change from baseline (*G*; $P < 0.05$, one way ANOVA; $n = 5$, 18, and 15) were also measured at 8 weeks after injection. *H*: Representative PAS staining was performed on paraffin-embedded kidney sections from sham-LMC, D-LMC, and D-podVEGFC mice. Scale bars = 25 μm. Representative Picro Sirius red immunohistochemistry images are demonstrated under bright-field (*I*) and polarized (*J*) lenses ($n = 3$). Magnification = ×40. *K*: PAS staining intensity is quantified using Quantity One ($P < 0.001$, one-way ANOVA, $n = 3$). Post hoc tests are indicated: *$P < 0.05$, **$P < 0.01$. D-podVC, D-podVEGFC.

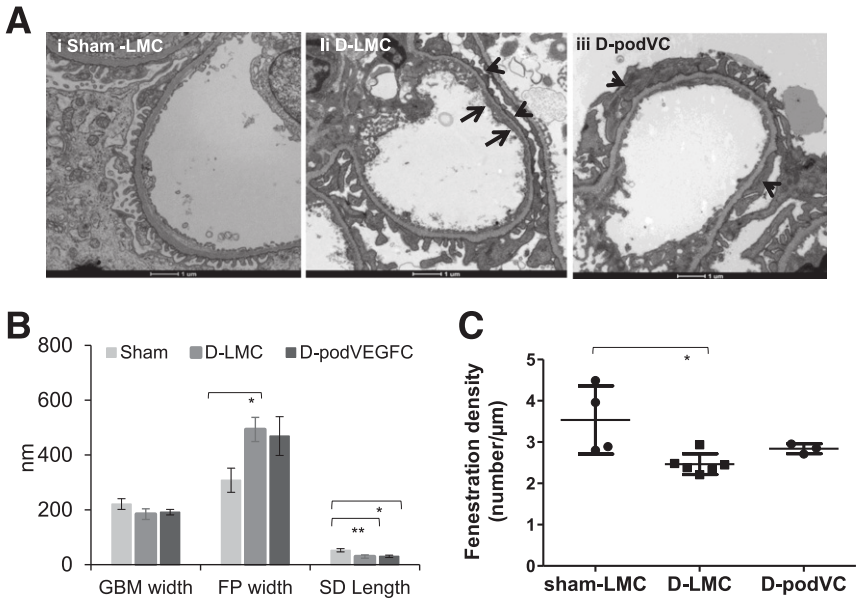

Figure 6—VEGFC intervention ameliorates early ultrastructural changes in DN. Mice given doxycycline at 4 weeks after STZ administration were cardiac perfusion fixed. Representative electron micrographs are shown at high power to show details of capillary loops in sham-LMC (*Ai*), D-LMC (*Aii*), and D-podVEGFC (D-podVC) (*Aiii*) mice. Arrows highlight reduced endothelial fenestration density, and arrowheads highlight flattened foot processes. Scale bars, 1 μm. *B*: Ultrastructural changes were quantified by measuring GBM width, podocyte foot process (FP) width ($P < 0.05$, one-way ANOVA), and slit diaphragm (SD) length ($n = 4$, 6, and 3, respectively; $P < 0.001$, one-way ANOVA). *C*: Endothelial fenestration density values per micrometer of GBM were also quantified ($P < 0.05$, one-way ANOVA). $n = 4$, 6, and 3. Bonferroni post hoc tests indicated: $^{*}P < 0.05$, $^{**}P < 0.01$.

by VEGFA and VEGFC. Interestingly, VEGFC also protected from a diabetes-induced increase in VEGF receptor expression in glomeruli. These data support previous observed increases in VEGFR2 expression in DN (57,58), although changes in glomerular VEGFR3 expression are not well documented. VEGFR2 and VEGFR3 expression were both reduced in D-podVEGFC mice; therefore, the potential for heterodimerization remains the same. However, the potential for receptor phosphorylation may be reduced, thereby reducing downstream signaling. Glomerular VEGFA is known to be upregulated in early DN (18) and most glomerular VEGF-receptor complexes are localized to GEnCs (18). This indicates that VEGFA predominantly regulates the endothelial phenotype during diabetic glomerulopathy, although endothelial cells are thought to "signal back" to the podocytes, inducing their injury (43). Hohenstein et al. (18) demonstrated that mildly injured glomeruli in early DN (relating to glomeruli in our study) had increased VEGFA-bound receptor complexes, whereas more severely injured glomeruli had decreased VEGFA-bound receptor complexes. Perhaps the key for VEGFC-mediated protection is to competitively reduce VEGFA receptor signaling, particularly in early DN.

VEGFC induces lymphatic hyperplasia and is associated with lymphangiomas and lymphangiosarcomas (59). Subcutaneous VEGFC overexpression also increases obesity and insulin resistance (60), and VEGFC is implicated in inflammation in late DN (61). Therefore, it is unlikely that VEGFC can be given therapeutically in its native form, although, of note, it was used successfully in mice to treat polycystic kidney disease (41) and to treat renal interstitial fibrosis for 14 days (62), and we gave VEGFC daily i.p. for a total of 7 days with no gross morphological effects. Lymphangiogenesis is increased in the tubular interstitium in DN (61), and this is considered a protective mechanism to aid drainage (63), but may also promote inflammation (64). If this mechanism is saturated, it can lead to edema in the kidney, as suggested by Uchiyama et al. (63). Importantly, in a model of unilateral ureteral obstruction, VEGFC treatment, by osmotic mini-pump, attenuated the infiltration of inflammatory cells (60). We have not yet investigated whether lymphangiogenesis is promoted in podVEGFC mice, but this is an important consideration in diabetes and is another potential reason for reduced hypertrophy in podVEGFC diabetic mice. Whether VEGFC can act as a microvascular protectant in other vascular beds in diabetes remains to be seen. In order to harness the effects of VEGFC therapeutically, it may be more appropriate to target the VEGFC signaling pathway. One such approach would be to target the VEGFR2/VEGFR3 complex as was done previously for VEGFR1/VEGFR2 complexes (65). Another approach would be to target signaling pathways that promote eGLX synthesis. If VEGFC can protect from diabetes-induced eGLX damage, then this is another exciting avenue of treatment. We have shown that VEGFC can protect against increased Ps'alb caused by systemic

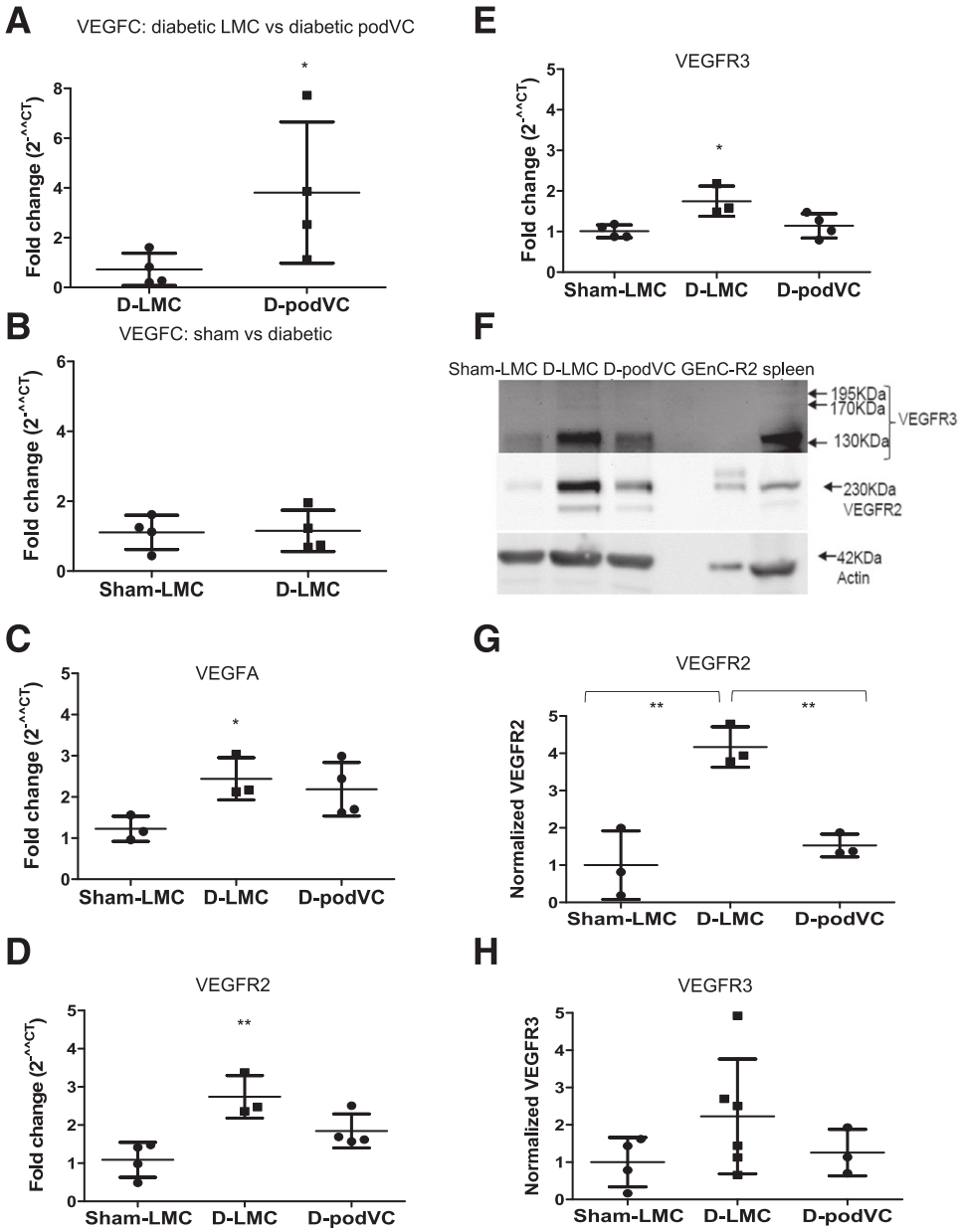

Figure 7—Glomerular VEGFC prevents the diabetes-associated changes in VEGFR expression. Glomeruli-enriched fractions from sham-LMC, D-podVEGFC (D-podVC), and D-LMC mice given doxycycline from 4 weeks after injection. mRNA was extracted and quantified using quantitative PCR normalized first to GAPDH then to LMC ($2^{-\Delta\Delta CT}$). Glomerular-enriched fraction VEGFC expression is demonstrated by QPCR in D-podVEGFC compared with D-LMC mice (i.e., overexpressed) (*A*; $P < 0.05$, unpaired *t* test; $n = 4$) and in D-LMC compared with sham mice (i.e., endogenous) (*B*; $n = 4$). Glomerular-enriched fraction VEGFA mRNA expression is demonstrated by quantitative PCR in sham-LMC, D-LMC, and D-podVEGFC mice (*C*; $P < 0.05$, one-way ANOVA; $n = 3$). Glomerular VEGFR2 (*D*; $P < 0.01$, one-way ANOVA; $n = 3$, 3, and 4) and VEGFR3 (*E*; $P < 0.05$, one-way ANOVA; $n = 3$, 3, and 4) expression in sham-LMC, D-LMC, and D-podVEGFC mice are shown. Expression changes at the protein level for VEGFR3 and VEGFR2 were confirmed by Western blotting in isolated glomeruli from the same groups of mice. *F*: VEGFR2 overexpressing GEnCs (GEnC-R2) and mouse spleen were used as positive controls for VEGFR2 and VEGFR3, respectively ($n = 3$). Normalized density to actin, then sham for VEGFR2 (*G*; $n = 3$; $P < 0.01$) and VEGFR3 (*H*; $n = 4$, 6, and 3, respectively) is shown. Bonferroni post hoc tests are indicated: $^*P < 0.05$, $^{**}P < 0.01$.

eGLX damage, both in chronic and acute models. We have also previously shown in vitro that VEGFA induced eGLX shedding in GEnC while VEGFC induced eGLX synthesis (33). As highlighted above, the D-podVEGFC mice did not experience significant fenestration density loss. The restoration of filtration control for albumin is potentially due to altered e-GLX coverage of the fenestrations. Since eGLX dysfunction is considered an early insult in DN (66), and the type 1 diabetes models used show an early phenotype, perhaps VEGFC mediates its protection

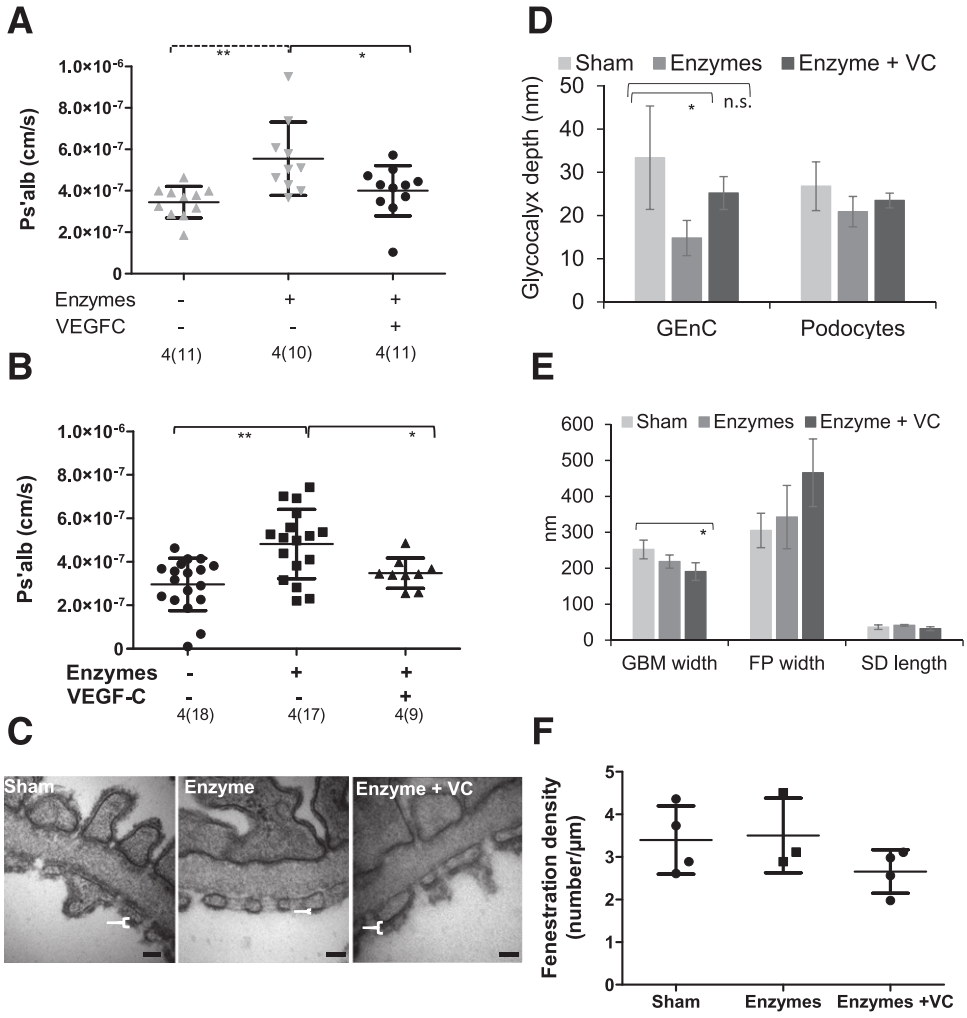

Figure 8—VEGFC protects against raised Ps'alb levels caused by systemic eGLX dysfunction. FVB/mixed background mice were administered hyaluronidase and chondroitinase either acutely (30 min i.v.; *A*) or chronically (osmotic minipump, 2 weeks; *B–F*). *A*: Glomeruli isolated from mice with acute eGLX dysfunction (enzymes +) were incubated ex vivo with (+) VEGFC, then Ps'alb was measured and compared with historical data without (−) VEGFC (40) (one-way ANOVA with Bonferroni post hoc tests indicated). Mice exposed to enzymes chronically over a period of 2 weeks were given VEGFC i.p. in the last week. *B*: Ps'alb measurements were taken in isolated glomeruli (one-way ANOVA, Bonferroni post hoc tests indicated). *C*: Representative electron microscope images of the glomerular filtration barrier for each condition (n = 4, 3, and 4, respectively) are shown with e-GLX highlighted (white brackets; scale bar, 100 nm). Glomerular ultrastructural parameters from these mice were quantified; eGLX depth, podocyte GLX depth (*D*; one-way ANOVA with Bonferroni post hoc tests indicated); GBM thickness (one-way ANOVA, Bonferroni post hoc tests indicated), podocyte foot process (FP) width, slit diaphragm (SD) length (*E*; $P < 0.05$, one way ANOVA, no post hoc test significance); and endothelial fenestration density (*F*) are shown. *$P < 0.05$ and **$P < 0.01$ (dashed lines indicate comparison with previously published data).

though eGLX restoration in early DN. This will be a focus of future work.

Importantly, we have demonstrated a novel role for VEGFC in the development of early DN.

Funding. This work was supported by a British Heart Foundation (BHF) Basic Science Intermediate Fellowship (FS/10/017/28249) (to M.G., N.R.B., S.L.B., and R.R.F.) and a BHF studentship and project grant (FS/13/9/29957 and PG/15/81/31740) (to K.L.O.); a Kidney Research UK project grant (RP45/2013) (to R.D.R.) and a studentship grant (ST5/2012) (to S.D.); a European Foundation for the Study of Diabetes grant (EFSD/Novartis Programme, 2014) (to K.B.B.); an Medical Research Council Clinician Scientist award (G0802829) (to A.H.J.S.); and a Diabetes Research Wellness Foundation grant (SCA/OF/12/13) (to R.R.F.).

Duality of Interest. No potential conflicts of interest relevant to this article were reported.

Author Contributions. K.L.O. helped to design the experiments, acquired data, interpreted the results, and approved the final version of the manuscript. M.G., N.R.B., S.L.B., K.B.B., S.D., B.P.D., R.D.R., and L.K.F. acquired data, interpreted the results, and approved the final version of the manuscript. C.R.N. advised on electron microscopy imaging and measurements and approved the final version of the manuscript. P.W.M., L.G., K.A., D.O.B., A.H.J.S., G.I.W., and S.C.S. helped to design the experiments, interpreted the results, and approved the final version of the manuscript. R.R.F. conceived and designed the work, interpreted the results, revised the manuscript, and approved the final version.

R.R.F. is the guarantor of this work and, as such, had full access to all the data in the study and takes responsibility for the integrity of the data and the accuracy of the data analysis.

References

1. Deckert T, Feldt-Rasmussen B, Borch-Johnsen K, Jensen T, Kofoed-Enevoldsen A. Albuminuria reflects widespread vascular damage. The Steno hypothesis. Diabetologia 1989;32:219–226
2. Polovina MM, Potpara TS. Endothelial dysfunction in metabolic and vascular disorders. Postgrad Med 2014;126:38–53
3. Dobre D, Nimade S, de Zeeuw D. Albuminuria in heart failure: what do we really know? Curr Opin Cardiol 2009;24:148–154
4. Viberti GC, Hill RD, Jarrett RJ, Argyropoulos A, Mahmud U, Keen H. Microalbuminuria as a predictor of clinical nephropathy in insulin-dependent diabetes mellitus. Lancet 1982;1:1430–1432
5. Haraldsson B, Nyström J, Deen WM. Properties of the glomerular barrier and mechanisms of proteinuria. Physiol Rev 2008;88:451–487
6. Satchell SC, Tooke JE. What is the mechanism of microalbuminuria in diabetes: a role for the glomerular endothelium? Diabetologia 2008;51:714–725
7. Malik AB, Lynch JJ, Cooper JA. Endothelial barrier function. J Invest Dermatol 1989;93(Suppl.):62S–67S
8. Clough G. Relationship between microvascular permeability and ultrastructure. Prog Biophys Mol Biol 1991;55:47–69
9. Curry FR. Microvascular solute and water transport. Microcirculation 2005;12:17–31
10. Regele HM, Fillipovic E, Langer B, et al. Glomerular expression of dystroglycans is reduced in minimal change nephrosis but not in focal segmental glomerulosclerosis. J Am Soc Nephrol 2000;11:403–412
11. van den Berg BM, Nieuwdorp M, Stroes ES, Vink H. Glycocalyx and endothelial (dys) function: from mice to men. Pharmacol Rep 2006;58(Suppl.):75–80
12. Bailey E, Bottomley MJ, Westwell S, et al. Vascular endothelial growth factor mRNA expression in minimal change, membranous, and diabetic nephropathy demonstrated by non-isotopic in situ hybridisation. J Clin Pathol 1999;52:735–738
13. Ostendorf T, Kunter U, Eitner F, et al. VEGF(165) mediates glomerular endothelial repair. J Clin Invest 1999;104:913–923
14. Satchell SC, Braet F. Glomerular endothelial cell fenestrations: an integral component of the glomerular filtration barrier. Am J Physiol Renal Physiol 2009;296:F947–F956
15. Salmon AH, Neal CR, Bates DO, Harper SJ. Vascular endothelial growth factor increases the ultrafiltration coefficient in isolated intact Wistar rat glomeruli. J Physiol 2006;570:141–156
16. Satchell SC, Anderson KL, Mathieson PW. Angiopoietin 1 and vascular endothelial growth factor modulate human glomerular endothelial cell barrier properties. J Am Soc Nephrol 2004;15:566–574
17. Bates DO. Vascular endothelial growth factors and vascular permeability. Cardiovasc Res 2010;87:262–271
18. Hohenstein B, Hausknecht B, Boehmer K, Riess R, Brekken RA, Hugo CP. Local VEGF activity but not VEGF expression is tightly regulated during diabetic nephropathy in man. Kidney Int 2006;69:1654–1661
19. Foster RR. The importance of cellular VEGF bioactivity in the development of glomerular disease. Nephron Exp Nephrol 2009;113:e8–e15
20. Yuan F, Chen Y, Dellian M, Safabakhsh N, Ferrara N, Jain RK. Time-dependent vascular regression and permeability changes in established human tumor xenografts induced by an anti-vascular endothelial growth factor/vascular permeability factor antibody. Proc Natl Acad Sci U S A 1996;93:14765–14770
21. McArthur K, Feng B, Wu Y, Chen S, Chakrabarti S. MicroRNA-200b regulates vascular endothelial growth factor-mediated alterations in diabetic retinopathy. Diabetes 2011;60:1314–1323
22. de Vriese AS, Tilton RG, Elger M, Stephan CC, Kriz W, Lameire NH. Antibodies against vascular endothelial growth factor improve early renal dysfunction in experimental diabetes. J Am Soc Nephrol 2001;12:993–1000
23. Braghiroli MI, Sabbaga J, Hoff PM. Bevacizumab: overview of the literature. Expert Rev Anticancer Ther 2012;12:567–580
24. Stewart MW. The expanding role of vascular endothelial growth factor inhibitors in ophthalmology. Mayo Clin Proc 2012;87:77–88
25. Frampton JE. Ranibizumab: in diabetic macular oedema. Drugs 2012;72:509–523
26. Eremina V, Jefferson JA, Kowalewska J, et al. VEGF inhibition and renal thrombotic microangiopathy. N Engl J Med 2008;358:1129–1136
27. Foster RR, Satchell SC, Seckley J, et al. VEGF-C promotes survival in podocytes. Am J Physiol Renal Physiol 2006;291:F196–F207
28. Bahram F, Claesson-Welsh L. VEGF-mediated signal transduction in lymphatic endothelial cells. Pathophysiology 2010;17:253–261
29. Nilsson I, Bahram F, Li X, et al. VEGF receptor 2/-3 heterodimers detected in situ by proximity ligation on angiogenic sprouts. EMBO J 2010;29:1377–1388
30. Cao R, Eriksson A, Kubo H, Alitalo K, Cao Y, Thyberg J. Comparative evaluation of FGF-2-, VEGF-A-, and VEGF-C-induced angiogenesis, lymphangiogenesis, vascular fenestrations, and permeability. Circ Res 2004;94:664–670
31. Robinson CJ, Stringer SE. The splice variants of vascular endothelial growth factor (VEGF) and their receptors. J Cell Sci 2001;114:853–865
32. Foster RR, Slater SC, Seckley J, et al. Vascular endothelial growth factor-C, a potential paracrine regulator of glomerular permeability, increases glomerular endothelial cell monolayer integrity and intracellular calcium. Am J Pathol 2008;173:938–948
33. Foster RR, Armstrong L, Baker S, et al. Glycosaminoglycan regulation by VEGFA and VEGFC of the glomerular microvascular endothelial cell glycocalyx in vitro. Am J Pathol 2013;183:604–616
34. Satchell SC, Tasman CH, Singh A, et al. Conditionally immortalized human glomerular endothelial cells expressing fenestrations in response to VEGF. Kidney Int 2006;69:1633–1640
35. Østergaard MV, Pinto V, Stevenson K, Worm J, Fink LN, Coward RJ. DBA2J db/db mice are susceptible to early albuminuria and glomerulosclerosis that correlate with systemic insulin resistance. Am J Physiol Renal Physiol 2017;312:F312–F321
36. Garner KL, Betin VMS, Pinto V, et al. Enhanced insulin receptor, but not PI3K, signalling protects podocytes from ER stress. Sci Rep 2018;8:3902
37. Shigehara T, Zaragoza C, Kitiyakara C, et al. Inducible podocyte-specific gene expression in transgenic mice. J Am Soc Nephrol 2003;14:1998–2003
38. Lohela M, Heloterä H, Haiko P, Dumont DJ, Alitalo K. Transgenic induction of vascular endothelial growth factor-C is strongly angiogenic in mouse embryos but leads to persistent lymphatic hyperplasia in adult tissues. Am J Pathol 2008;173:1891–1901
39. Oltean S, Qiu Y, Ferguson JK, et al. Vascular endothelial growth factor-A165b is protective and restores endothelial glycocalyx in diabetic nephropathy. J Am Soc Nephrol 2015;26:1889–1904
40. Desideri S, Onions KL, Qiu Y, et al. A novel assay provides sensitive measurement of physiologically relevant changes in albumin permeability in isolated human and rodent glomeruli. Kidney Int 2018;93:1086–1097
41. Huang JL, Woolf AS, Kolatsi-Joannou M, et al. Vascular endothelial growth factor C for polycystic kidney diseases. J Am Soc Nephrol 2016;27:69–77
42. Takemoto M, Asker N, Gerhardt H, et al. A new method for large scale isolation of kidney glomeruli from mice. Am J Pathol 2002;161:799–805
43. Eremina V, Sood M, Haigh J, et al. Glomerular-specific alterations of VEGF-A expression lead to distinct congenital and acquired renal diseases. J Clin Invest 2003;111:707–716
44. Dixelius J, Makinen T, Wirzenius M, et al. Ligand-induced vascular endothelial growth factor receptor-3 (VEGFR-3) heterodimerization with VEGFR-2 in primary lymphatic endothelial cells regulates tyrosine phosphorylation sites. J Biol Chem 2003;278:40973–40979
45. Lytvyn Y, Perkins BA, Cherney DZ. Uric acid as a biomarker and a therapeutic target in diabetes. Can J Diabetes 2015;39:239–246

46. Cooper ME, Vranes D, Youssef S, et al. Increased renal expression of vascular endothelial growth factor (VEGF) and its receptor VEGFR-2 in experimental diabetes. Diabetes 1999;48:2229–2239
47. Dane MJ, van den Berg BM, Lee DH, et al. A microscopic view on the renal endothelial glycocalyx. Am J Physiol Renal Physiol 2015;308:F956–F966
48. Dessapt-Baradez C, Woolf AS, White KE, et al. Targeted glomerular angiopoietin-1 therapy for early diabetic kidney disease. J Am Soc Nephrol 2014;25:33–42
49. Oltean S, Qiu Y, Ferguson JK, et al. Vascular endothelial growth factor-A165b is protective and restores endothelial glycocalyx in diabetic nephropathy. J Am Soc Nephrol 2015;26:1889–1904
50. Toyoda M, Najafian B, Kim Y, Caramori ML, Mauer M. Podocyte detachment and reduced glomerular capillary endothelial fenestration in human type 1 diabetic nephropathy. Diabetes 2007;56:2155–2160
51. Weil EJ, Lemley KV, Mason CC, et al. Podocyte detachment and reduced glomerular capillary endothelial fenestration promote kidney disease in type 2 diabetic nephropathy. Kidney Int 2012;82:1010–1017
52. Satchell SC. The glomerular endothelium emerges as a key player in diabetic nephropathy. Kidney Int 2012;82:949–951
53. Marshall CB. Rethinking glomerular basement membrane thickening in diabetic nephropathy: adaptive or pathogenic? Am J Physiol Renal Physiol 2016; 311:F831–F843
54. Hu C, Sun L, Xiao L, et al. Insights into the mechanisms involved in the expression and regulation of extracellular matrix proteins in diabetic nephropathy. Curr Med Chem 2015;22:2858–2870
55. Baines RJ, Brunskill NJ. Tubular toxicity of proteinuria. Nat Rev Nephrol 2011; 7:177–180
56. Gavard J, Patel V, Gutkind JS. Angiopoietin-1 prevents VEGF-induced endothelial permeability by sequestering Src through mDia. Dev Cell 2008;14:25–36
57. Jin J, Peng C, Wu SZ, Chen HM, Zhang BF. Blocking VEGF/Caveolin-1 signaling contributes to renal protection of fasudil in streptozotocin-induced diabetic rats. Acta Pharmacol Sin 2015;36:831–840
58. Yang KS, Lim JH, Kim TW, et al. Vascular endothelial growth factor-receptor 1 inhibition aggravates diabetic nephropathy through eNOS signaling pathway in db/db mice. PLoS One 2014;9:e94540
59. Lohela M, Saaristo A, Veikkola T, Alitalo K. Lymphangiogenic growth factors, receptors and therapies. Thromb Haemost 2003;90:167–184
60. Karaman S, Hollmén M, Yoon SY, et al. Transgenic overexpression of VEGF-C induces weight gain and insulin resistance in mice. Sci Rep 2016;6: 31566
61. Sakamoto I, Ito Y, Mizuno M, et al. Lymphatic vessels develop during tubulointerstitial fibrosis. Kidney Int 2009;75:828–838
62. Hasegawa S, Nakano T, Torisu K, et al. Vascular endothelial growth factor-C ameliorates renal interstitial fibrosis through lymphangiogenesis in mouse unilateral ureteral obstruction. Lab Invest 2017;97:1439–1452
63. Uchiyama T, Takata S, Ishikawa H, Sawa Y. Altered dynamics in the renal lymphatic circulation of type 1 and type 2 diabetic mice. Acta Histochem Cytochem 2013;46:97–104
64. Yazdani S, Navis G, Hillebrands JL, van Goor H, van den Born J. Lymphangiogenesis in renal diseases: passive bystander or active participant? Expert Rev Mol Med 2014;16:e15
65. Cudmore MJ, Hewett PW, Ahmad S, et al. The role of heterodimerization between VEGFR-1 and VEGFR-2 in the regulation of endothelial cell homeostasis. Nat Commun 2012;3:972
66. Dedov I, Shestakova M, Vorontzov A, Palazzini E. A randomized, controlled study of sulodexide therapy for the treatment of diabetic nephropathy. Nephrol Dial Transplant 1997;12:2295–2300